Molecular Neurobiology (2025) 62:2587–2600
https://doi.org/10.1007/s12035-024-04420-0

RESEARCH

CircKat6b Mediates the Antidepressant Effect of Esketamine by Regulating Astrocyte Function

Na Hu[1,2] · Yujie Zheng[1,2] · Xueru Liu[1,2] · Jing Jia[2] · Jianguo Feng[2] · Chunxiang Zhang[2] · Li Liu[1,2] · Xiaobin Wang[1,2]

Received: 13 May 2024 / Accepted: 5 August 2024 / Published online: 14 August 2024

Abstract

The abundant expression of circular RNAs (circRNAs) in the central nervous system and their contribution to the pathogenesis of depression suggest that circRNAs are promising therapeutic targets for depression. This study explored the role and mechanism of *circKat6b* in esketamine's antidepressant effect. We found that intravenous administration of esketamine (5 mg/kg) treatment decreased the *circKat6b* expression in the astrocytes of hippocampus induced by a chronic unpredictable mild stress (CUMS) mouse model, while the overexpression of *circKat6b* in the hippocampus significantly attenuated the antidepressant effects of esketamine in depressed mice. RNA-sequencing, RT-PCR, and western blot experiments showed that the stat1 and p-stat1 expression were significantly upregulated in mouse astrocytes overexpressing *circKat6b*. In the CUMS mouse model, overexpression of *circKat6b* in the hippocampus significantly reversed the downregulation of p-stat1 protein expression caused by esketamine. Our findings demonstrated that a novel mechanism of the antidepressant like effect of esketamine may be achieved by reducing the expression of *circKat6b* in the astrocyte of the hippocampus of depressed mice.

Keywords Astrocytes · circRNAs · Esketamine · Hippocampus · Stat1

Introduction

Major depressive disorder (MDD) is a prevalent and enduring mental disorder that impacts approximately 300 million individuals within the global population [1]. Conventional antidepressants have drawbacks such as delayed onset of therapeutic effects, adverse reactions, and limited efficacy in approximately 30% of treated individuals [2]. Esketamine is the S-enantiomer of ketamine (R,S-ketamine) that has a rapid and obvious antidepressant effect [3]. On March 4, 2019, the US Food and Drug Administration (FDA) approved a nasal spray form of esketamine for treating adult patients with treatment-resistant depression (TRD) [4]. However, the negative side effects of esketamine include psychotic and transient dissociative symptoms [5], and hence, a comprehensive understanding of the mechanisms underlying its antidepressant effects is required to facilitate the identification of more efficacious therapeutic targets and advance novel antidepressant interventions with reduced adverse effects.

CircRNAs represent a distinct class of non-coding RNA molecules characterized by the absence of both a 5′ cap structure and a 3′ polyadenylated tail, instead possessing a covalently closed circular configuration. They exhibit a broad distribution [6], are highly conserved [7], and demonstrate tissue-specificity throughout the developmental process [8]. CircRNAs generated from the cyclization of exons are mostly distributed in the cytoplasm and have post transcriptional regulation function [9]. Research showed that circRNAs were closely related to the pathogenesis of various diseases, among which they played a crucial role in regulating the physiological and pathological processes of the nervous system, including neural development and plasticity, cell growth, Alzheimer's disease, and depression [10–12]. Our previous study showed that the levels of rno-circRNA-005442 and rno-circRNA-014900 were reported to be significantly reduced in the hippocampus of

Na Hu and Yujie Zheng contributed equally to this work.

✉ Xiaobin Wang
wangxiaobin67@163.com

[1] Department of Anesthesiology, The Affiliated Hospital, Southwest Medical University, Luzhou 646000, Sichuan Province, China

[2] Anesthesiology and Critical Care Medicine Key Laboratory of Luzhou, The Affiliated Hospital, Southwest Medical University, Luzhou 646000, Sichuan Province, China

rats after treatment with sub-anesthetic doses of ketamine, and rno-circRNA-005442 was shown to form via cyclization of an exon in the rat *Kat6b* gene [13]. However, the mechanism of *circKat6b* in the antidepressant effect of esketamine is unclear.

Research indicated that the antidepressant efficacy of esketamine is significantly associated with its anti-inflammatory impact on the central nervous system (CNS) [14, 15]. Microglia and astrocytes are identified as the main contributors to CNS inflammation, with research indicating that dysfunction of astrocytes may be a significant factor in the development of depression [14]. Evidence showed that astrocyte dysfunction can lead to excessive inflammatory response in the brain, releasing inflammatory factors and chemokines such as interleukin-6 (IL-6), tumor necrosis factor-α (TNF-α), inducible nitric oxide synthase (iNOS), and C–C motif chemokine ligand 2 (CCL2), thereby aggravating central nervous system damage and participating in the pathological process of depression [16]. Clinical studies have found that alterations in astrocyte function and morphology were discernible in the brains of depression patients, alongside a notable upregulation of pro-inflammatory factors and chemokines in the serum and cerebrospinal fluid of depressed patients [17]. The hippocampus of CUMS mice exhibited a notable decrease in the expression of the astrocyte marker glial fibrillary acidic protein (GFAP), as well as a significant reduction in the number of cells displaying positive GFAP expression [18, 19]. The JAK-STAT signaling pathway is a well-established mechanism involved in the inflammatory response, and its key constituents are extensively distributed throughout the cerebral cortex and hippocampal tissue [20]. An analysis of protein–protein interaction networks indicated that the activation of JAK-STAT signaling is a significant pathway that contributes to immune impairments in individuals with major depressive disorder [21], and activation of stat1 induced astrocytes to produce inflammatory factors, chemokines, and other factors involved in the inflammatory response of the nervous system [22, 23], suggesting that stat1 plays an important role in astrocyte-mediated neuroinflammation. Our previous study showed that miR-221-3p directly targeted interferon regulatory factor 2 (IRF2) to upregulate interferon alpha (IFN-α) expression in astrocytes and thus participated in the antidepressant effects of ketamine [24], implying that miRNAs also play an important role in the inflammatory pathway in astrocytes. With further research, it was found that not only miRNAs but also long non-coding RNAs (lncRNAs), circRNAs, and other non-coding RNAs exert a regulatory influence on central nervous system inflammation [25, 26]. Thus, the potential involvement of *circKat6b* in the antidepressant effects of esketamine via stat1-mediated neuroinflammatory responses in astrocytes remains uncertain.

In the present study, we made a novel discovery that esketamine reduced the expression level of *circKat6b* in hippocampal astrocytes of depressive-like mice. The antidepressant properties of esketamine were attenuated by the overexpression of *circKat6b*, which effectively counteracted its inhibitory effects on inflammatory factors within the hippocampus of CUMS mice. Furthermore, the regulatory role of *circKat6b* in astrocyte function was found to involve stat1. Our study provides evidence of the significant involvement of *circKat6b* in the antidepressant properties of esketamine, thereby suggesting that *circKat6b* may be a promising therapeutic target for depression treatment.

Materials and Methods

Animals

Male C57BL/6 J mice weighing 20.0 g and 26.0 g and aged 6–8 weeks were procured from Chongqing Tengxin, a Chinese supplier. The mice were randomly assigned to different experimental groups and were maintained under a controlled temperature (22 °C ± 2 °C) and humidity (50% ± 20%) with a 12/12-h light/dark cycle (lights on at 7:00 a.m.). This study complied with the guidelines of the Animal Ethics Committee of the Affiliated Hospital of Southwest Medical University (approval number: SWMU20220087).

CUMS Protocol and Behavioral Tests

As shown in Fig. 1 (Experiment 1), depressive-like behavior was induced in mice using the CUMS protocol as previously described [27]. The mice were subjected to experimental stressors in a randomized sequence over 21 days, ensuring that each stressor was not administered for two consecutive days and was limited to a maximum of twice per week. Significant variations in depression-like behaviors obtained on experimental days 22–25 compared to those of the control group were used to judge whether the CUMS model had been successfully established. The antidepressant effect of esketamine was assessed by behavioral testing 24 h after a single dose of esketamine (5 mg/kg, dissolved in 0.9% saline 100 μL, tail vein injection; batch number: H20193336, Minsheng Pharma Holdings, China). Each test was conducted by the same rater between the hours of 9:00 and 17:00 in a soundproofed environment with dim lighting, followed by subsequent evaluation. Prior to testing, the mice were acclimated to the testing room for a minimum duration of 3 h. Animals completed the sucrose preference test (SPT), tail suspension test (TST), and forced swim test (FST) as described in the previous study [27]. After the last

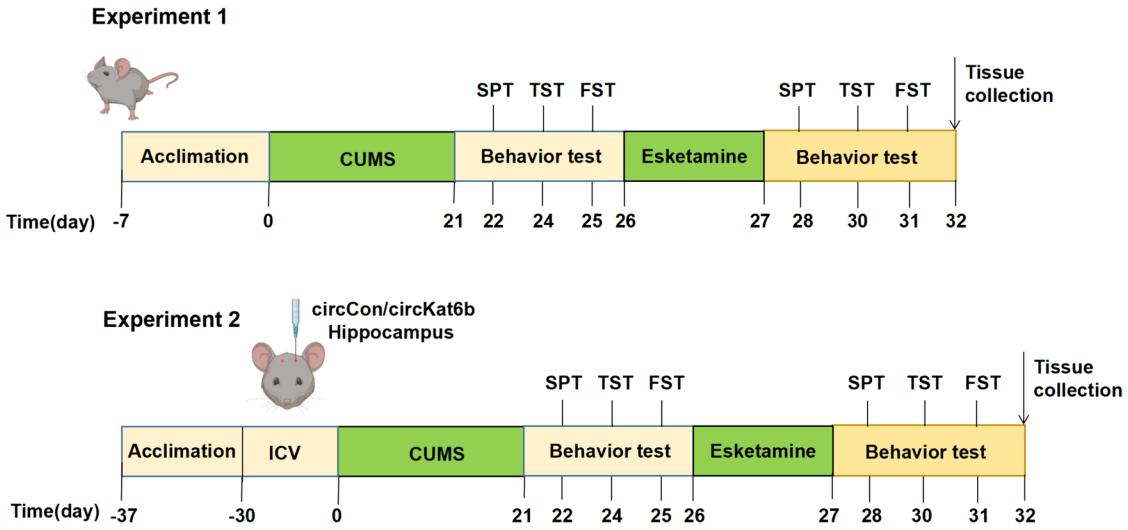

Fig. 1 Experimental design. CUMS, chronic unpredictable mild stress; SPT, sucrose preference test; FST, forced swim test; TST, tail suspension test; ICV, intracerebroventricular injection

behavioral test was completed, mice from each group were decapitated under 1% sodium pentobarbital (40 mg/kg, ip) anesthesia, and bilateral hippocampus was taken out on ice and immediately cooled in liquid nitrogen tanks, then stored in − 80 °C refrigerators.

Overexpression of *circKat6b* in the *Hippocampus* of Mice Using Adeno-associated Virus (AAV) and Microinjection

As shown in Fig. 1 (Experiment 2), the AAV-mediated vectors used in this study were procured from Hanbio Biotechnology (Shanghai, China). The company executed subsequent protocols to produce the viral vectors, which were derived from the primary pHBAAV-GFAP-EGFP plasmid that features an astrocyte-specific promoter and the selected AAV9 serotype. The coding sequence of the *circKat6b* (circbank: mmu-circ-0000505) was amplified and integrated into the pHBAAV-GFAP-EGFP vector using EcoRI and HindIII. The pHBAAV-GFAP-EGFP plasmid served as a control. The recombinant plasmid (pHBAAV-GFAP-circKat6b-EGFP) was co-transfected into 293 T cells with the pAAV-RC plasmid and pAAV helper for 72 h for viral packaging. Following transfection, AAV-293 T cells were harvested and subjected to freeze–thaw cycles and centrifugation. The resulting supernatant was purified using a Biomiga Adeno-Associated Virus Purification Kit (V1469-01). The final purified circControl-AAV or circKat6b-AAV viruses were collected and stored at − 80 °C. We next established the *circKat6b* overexpression mouse model on day 30 before CUMS, as previously described [28]. Specifically, male C57BL/6 J mice were subjected to bilateral microinjections of either circControl-AAV or *circKat6b*-AAV (1 µL 1×10^{12} vg/mL, Hanbio, China) into the hippocampus. The AAV vectors were stereotaxically injected into the bilateral hippocampus area (AP-2.0 mm, ML ± 1.0 mm, DV 2.0 mm) at a rate of 0.5 µL /min, with the needle being retained in place for 5 min before being gradually removed. Following suturing of the skin incision, the mice were individually housed in cages after regaining consciousness.

Cell Culture and Treatment

Astrocytes (C8D1A), microglia (BV2), and neurons (HT22) were obtained from the Chinese Academy of Sciences stem cell bank. The cells were cultured in DMEM (GBICO, USA) supplemented with 10% fetal bovine serum (PEAK SERUM, US), penicillin (100 U/mL), and streptomycin (100 µg/mL) in a 5% CO_2 atmosphere at 37 °C. To detect the effect of esketamine in vitro, the cells were treated with 25 µM of esketamine (Figure S1). Total RNA was extracted from C8D1A cells using the TRIzol reagent (Ambion, USA), and the cells were divided into two groups. In one group, the RNA was pretreated with RNase R (Beyotime, China) at a concentration of 3 U/µg RNA at 37 °C for 30 min, followed by inactivation at 70 °C for 10 min. The remaining group served as controls. RT-PCR was conducted to assess the expression of *circKat6b* and *β-actin*, both with and without RNase R treatment.

Cell Transfection

The gene sequences of *circKat6b* were obtained from NCBI, and a pair of primers were designed based the *Kat6b* gene sequences: forward 5′-CGGAATTCTAAT ACTTTCAGGTCTTGGTTTCCTAAAGATG-3′ and

reverse 5′-CGTGATCAAGTTGTTCTTACCTGGTCT TTCTCATGGGGTA-3′. The interference segment was ligated into the pCDH5-circRNA-copGFP-Puro cloning vector (pCDH5-copGFP) to construct the *circKat6b* overexpression vector (pCDH5-circKat6b). To generate the recombinant lentivirus LV-circKat6b, 293 T cells were co-transfected with 2 μg pCDH5-circKat6b plasmid, 0.5 μg VSVG plasmid, and 1.5 μg DVPR plasmid in 8 μL jetPRIME transfection reagent. The lentivirus supernatants were collected 48 h and 72 h after transfection. The stably transfected cells were selected using 5 μg/mL puromycin 72 h after infection with the lentiviral supernatant, and C8D1A cells with stable *circKat6b* overexpression were validated by RT-PCR.

RNA Extraction and RT-PCR

Total RNA from cells or animal tissues was isolated using TRIzol reagent according to the manufacturer's instructions (Ambion). Then, 1 μg of RNA was used for cDNA synthesis using the HiScript III 1st Strand cDNA Synthesis Kit (+ gDNA wiper) (Vazyme, China). PowerUp SYBR Green Master Mix (Thermo Fisher Scientific) was used to conduct qRT-PCR with QuantStudio 5 Applied Biosystems (Thermo Fisher Scientific). The fold-change in the expression of the target gene was determined using the comparative Ct approach (2-ΔΔCt method) with *β-actin* as the housekeeping gene. The primer sequences used for qRT-PCR are listed in Table 1.

The RNA levels of *circKat6b*, *GABAB1*, and *stat1* were detected using the following RT-PCR method: 94 °C for 3 min, and then 35 cycles of 94 °C for 30 s, 55 °C for 30 s, and 72 °C for 30 s. The reactions included DNA polymerase (Tiangen Biotech Co. Ltd. Beijing, China) and specific primers (Table 1) and was performed in a MyCycler thermal cycler (Bio-Rad, Hercules, CA, USA).

Table 1 RT-PCR primers

Primer name	Sequence
Mouse-circKat6b-F	AATGGGAGGTTACTGAAGGA
Mouse-circKat6b-R	AAGCAACAGCATAGGGACAA
Mouse-Kat6b-F	ACAACAACAGGGGGACACAA
Mouse-Kat6b-R	CCGCATGGCAGATTCTCTCT
Mouse-stat1-F	GATCGCTTGCCCAACTCTTG
Mouse-stat1-R	ACTGTGACATCCTTGGGCTG
Mouse-GABAB1-F	CGGGTGGATTTCCGATGTGA
Mouse-GABAB1-R	TGTGGCGTTCGATTCACCTG
Mouse-β-actin-F	CCTAAGGCCAACCGTGAAAA
Mouse-β-actin-R	GAGGCATACAGGGACAGCACA

The PCR products were separated in a 1.5% agarose gel by electrophoresis.

RNA Sequencing Library Construction and RNA-seq

Total RNA was extracted from C8D1A cells expressing pCDH5-copGFP or pCDH5-circKat6b using TRIzol reagent as described. An initial input of 1 μg total RNA was used to construct each sequencing library. All purified libraries were then sequenced on the Illumina Novaseq 6000 platform at Majorbio Corporation to generate 300-bp paired-end sequence reads. Three replicates were sequenced for each group, and differentially expressed genes (DEGs) were identified using the DESeq2 package with a threshold of adjusted P-value < 0.05 and |log2 fold change (FC)|≥ 1.

Immunofluorescence Staining andFluorescenceIn SituHybridization(FISH)

Immunofluorescence assays were performed as described previously [27]. C8D1A cells were cultured on coverslips and fixed with 4% paraformaldehyde (PFA) for 10 min, washed with PBS three times for 5 min each, and processed to detect circKat6b expression following the manufacturer's instructions (RiboBio). Images were captured using a microscope (ZEISS, Germany, ls810). The sequence of the probe used for detecting mouse *circKat6b* was 5′-FITC-CAUCUU UAGGAAACCAAGACCUGGUCUUUCUCAUG-3′, with biotinylation at the 5′ terminus.

Western Blot and Enzyme-Linked Immunosorbent Assay (ELISA)

Equal amounts of protein lysates were resolved by SDS-PAGE and transferred onto a nitrocellulose membrane. The membranes were incubated with the primary antibodies at 4 °C overnight and then hybridized with the corresponding secondary antibodies at room temperature for 1 h. Then, the protein bands were visualized using the ECL western blotting substrate (Solarbio, Beijing, China). The primary antibodies used were GFAP (Proteintech, 1:10000), GABAB1 (Abcam, 1:100), Stat1 (Proteintech, 1:2000), Phosphor-stat1 (Ser727) (Cell Signaling Technology, 1:1000), and β-actin (Proteintech, 1:5000). Hippocampal tissue was homogenized in RIPA lysis buffer, and the total protein lysate was collected by centrifugation at 12,000 rpm at 4℃ for 15 min. CCL-2, IL-6, iNOS and TNF-α levels were measured in the supernatants from hippocampal tissues using an ELISA kit according to the manufacturer's instructions (#ZC-38588, #ZC-37988, #ZC-38979, #ZC-39024; ZCIBIO, China).

Statistical Analyses

Statistical analyses were performed using GraphPad Prism 7 software. Significance was determined using Student's *t*-test for comparisons between two groups. One-way analysis of variance (ANOVA) and two-way ANOVA, followed by Tukey's test, were used for multigroup comparisons. All data are presented as the mean ± SEM. Statistical analyses performed for different experiments are described in the respective figure legends, and the results were considered significant at $P < 0.05$.

Results

Esketamine Decreases *circKat6b* Expression in the Hippocampus of CUMS Mice

Sequencing analysis revealed that rno-circRNA-005442 was homologous to *Kat6b*, with high species homology (Fig. 2A). This circular RNA was formed by the circularization of exon 3 of the human *Kat6b* gene or exon 2 of the mouse *Kat6b* gene (Fig. 2B). The use of divergent and convergent primers in the amplification of *circKat6b* demonstrated that the head-to-tail junction-specific primers could only amplify *circKat6b* cDNA, but not genomic DNA, confirming that *circKat6b* molecules had circular structures (Fig. 2C). The *circKat6b* was resistant to ribonuclease R digestion, whereas linear *Kat6b* mRNA was easily degraded (Fig. 2D).

CUMS mice showed a significant decrease in sugar water preference (Fig. 2E, $P < 0.001$) and an increase in immobility time (Fig. 2F and G, $P < 0.01$), which were accompanied by the upregulation of *circKat6b* expression in the hippocampus (Fig. 2H, $P < 0.001$). Intravenous administration of esketamine (5 mg/kg) treatment of CUMS mice significantly increased the sugar water preference rate (Fig. 2E, $P < 0.001$) and decreased the immobility time (Fig. 2F and G, $P < 0.01$), which correlated with the downregulation of *circKat6b* expression (Fig. 2H, $P < 0.05$).

CircKat6b Attenuates Esketamine Antidepressant Efficacy in CUMS Mice

After 1 month of AAV injection, the expression of green fluorescent protein (GFP) adeno-associated virus was predominantly localized within the entire hippocampus (Fig. 3A), while the expression of *circKat6b* significantly increased in the hippocampus (Fig. 3B,$P < 0.01$). Our data showed that both CUMS-circCon and CUMS-circKat6b groups of mice exhibited symptoms of depression when compared to the control group (Fig. 3C–E, $P < 0.01$). Whereas intravenous administration of esketamine(5 mg/kg) treatment increased sucrose preference of CUMS-circCon group and decreased immobility time in the FST and TST (Fig. 3C–E, $P < 0.05$), however, these effects were attenuated in mice overexpressing *circKat6b* when compared with the CUMS + Es-circCon group (Fig. 3C–E, $P < 0.01$).

CircKat6b Reduced the Beneficial Effect of Esketamine on Astrocyte Dysfunction in CUMS Mice

The highest level of basal *circKat6b* expression was observed in untreated C8D1A cells (Figure S2A, $P < 0.05$). Following a 24-h treatment with 25 μM esketamine, the expression of *circKat6b* was significantly downregulated in the C8D1A cells (Figure S2B, $P < 0.05$), while no significant changes were observed in the HT22 and BV2 cells. The expression of *circKat6b* in C8D1A cells was further confirmed using in situ hybridization, which revealed the predominant cytoplasmic localization of *circKat6b* in C8D1A cells (Figure S2C). The CUMS-circCon and CUMS-circKat6b mice had increased expression levels of CCL2 (Fig. 4A, $P < 0.01$), IL-6 (Fig. 4B, $P < 0.01$), iNOS (Fig. 4C, $P < 0.01$), and TNF-α (Fig. 4D, $P < 0.01$) inflammatory factors when compared with the control group (Fig. 4A–D). However, *circKat6b* overexpression resulted in a significant reduction in the inhibitory effect of esketamine on the expression of these inflammatory factors (Fig. 4A–D, $P < 0.01$). Immunofluorescence analysis revealed that the number of astrocytes in the hippocampus was significantly reduced in both groups of CUMS mice when compared to that of the control group (Fig. 4E and F, $P < 0.01$), while the overexpression of *circKat6b* effectively reduced the increase in astrocytes in the CUMS-circCon group treated with esketamine (Fig. 4E and F, $P < 0.01$). This finding was further confirmed by western blot analysis of GFAP. The expression levels of GFAP were notably decreased in the hippocampus of mice in the CUMS-circCon and CUMS-circKat6b groups compared with the control group (Fig. 4G and H, $P < 0.01$). And overexpression of *circKat6b* significantly inhibited the upregulation of GFAP expression in the CUMS-circCon group by esketamine (Fig. 4G and H, $P < 0.01$).

CircKat6b Regulates Stat1 Expression in Astrocytes

Astrocytes stably overexpressing *circKat6b* were established (Figure S3) to conduct a comprehensive transcriptome analysis. We found that the overexpression of *circKat6b* resulted in the upregulation of 266 genes and the downregulation of 200 genes in the transcripts (Fig. 5A; details of the top 20 DEGs are shown in Tables S1-S2). Gene ontology (GO) analysis revealed that most of the differentially expressed genes (DEGs) were enriched in "immune system process" and "response to stimulus" categories, which are associated

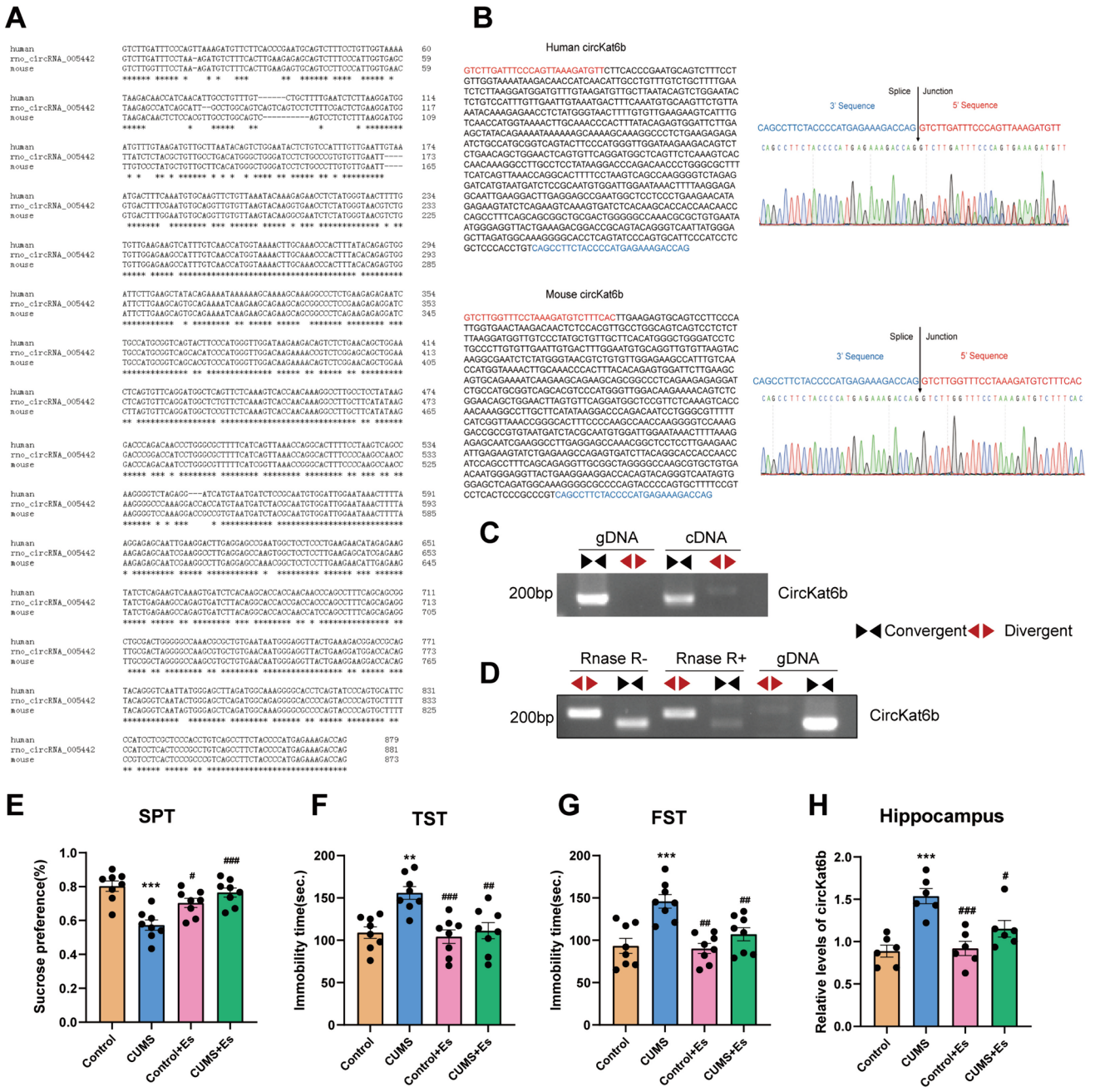

Fig. 2 Identification of *circKat6b*. **A** Sequence alignment of human, rat, and mouse *circKat6b*. Asterisk (*) represents the same base. **B** The circular sequence of human and mouse *circKat6b*. **C** RT-PCR amplification of linear and circular *Kat6b*. **D** Treated with RNase R (20 U/μL) for 1 h, *circKat6b*, linear *Kat6b* levels were detected by RT-PCR. Convergent, convergent primers for amplification of linear RNA. Divergent, divergent primers for amplification of circRNA. **E–G** SPT, TST, and FST were performed after a single dose of 5 mg/kg esketamine ($N=8$). **H** Relative *circKat6b* expression levels of hippocampus ($N=6$). Data represent the mean ± SEM. Statistical analysis of experimental conditions vs control group, $^{**}P<0.01$, $^{***}P<0.001$; vs CUMS group, $^{\#}P<0.05$, $^{\#\#}P<0.01$, $^{\#\#\#}P<0.001$ using two-way ANOVA followed by Tukey's test

with depression [29, 30] (Fig. 5B). Moreover, the KEGG and reactome enrichment analysis demonstrated that the DEGs between the pCDH5-circKat6b and pCDH5-copGFP groups were highly associated with several pathways, including the "ABC transporters," "NOD-like receptor signaling pathway," "PI3K-Akt signaling pathway," "GABA receptor activation," "GABAB receptor activation," and "Activation of GABAB receptors" (Fig. 5C and D). Finally, among the top 20 upregulated genes, *stat1* was significant associated with immunoinflammatory responses, and among the top

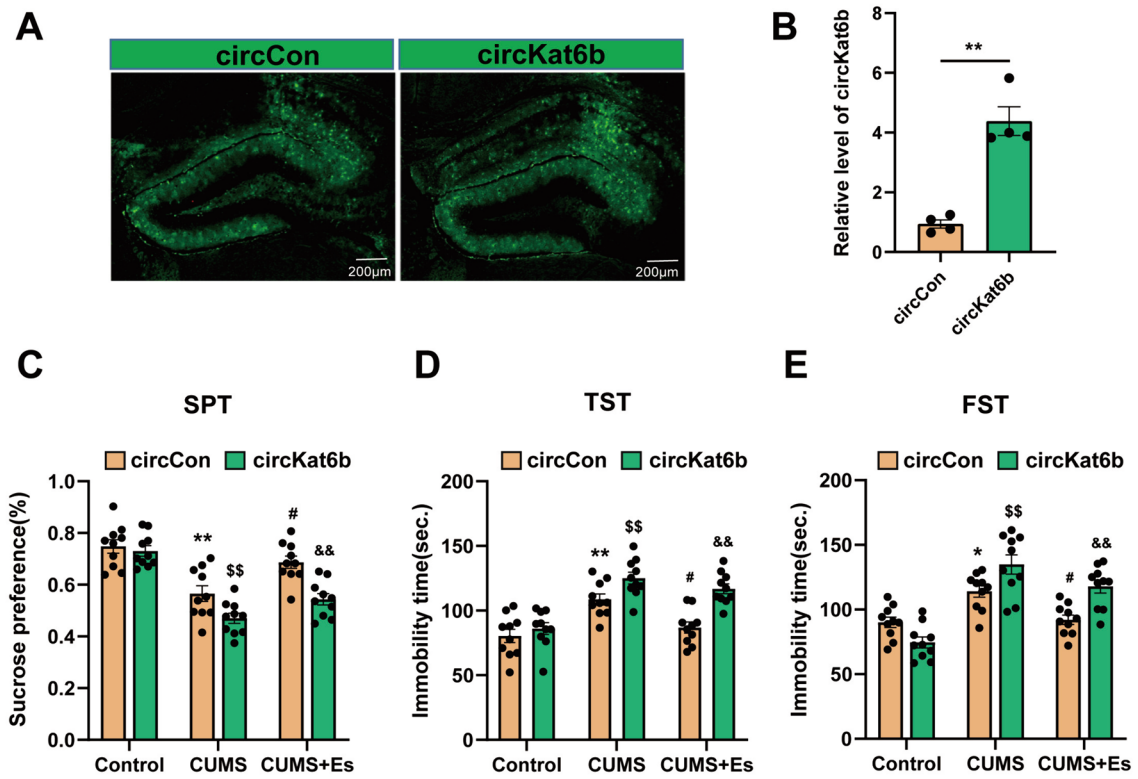

Fig. 3 *CircKat6b* mediates the antidepressant effect of esketamine. **A** The expression of *circKat6b* in the hippocampus visualized with immunofluorescence. Scale bar = 200 μm. **B** qRT-PCR results of *circKat6b* expression in the hippocampus ($N = 4$), with statistical analyses of experimental results vs circCon group, $^{**}P < 0.01$ using Student's *t*-test. **C**–**E** Effects of *circKat6b* AAV microinjection on depressive-like behaviors in CUMS mice. SPT, TST, and FST were measured at the end of CUMS modeling and after a single injection of 5 mg/kg esketamine ($N = 10$). vs control-circCon group, $^{*}P < 0.05$, $^{**}P < 0.01$; vs control-circKat6b group, $^{\$\$}P < 0.01$; vs CUMS-circCon group, $^{\#}P < 0.05$; vs CUMS + Es-circCon group, $^{\&\&}P < 0.01$ using two-way ANOVA followed by Tukey's test

20 downregulated genes, *GABAB1* was strongly associated with GABAB receptor activation. Our results demonstrated that *stat1* expression significantly increased at both the transcriptional and protein levels following the overexpression of *circKat6b*, while no significant change in the *GABAB1* expression was observed (Fig. 5E and F, $P > 0.05$).

CircKat6b Increases p-Stat1 Level to Reduce Esketamine Effects on Astrocyte Dysfunction in CUMS Mice

Our data revealed a significant upregulation of p-stat1 protein expression in the hippocampus of CUMS mice when compared to that of the control group (Fig. 6A, $P < 0.01$). Following intravenous administration of esketamine (5 mg/kg) treatment, the expression of p-stat1 was downregulated (Fig. 6A; $P < 0.05$); however, the overexpression of *circKat6b* effectively attenuated the decrease in p-stat1 protein expression observed in the esketamine-treated CUMS-circCon group (Fig. 6B, $P < 0.01$). Immunofluorescent labeling provided additional evidence of nuclear enrichment of stat1 in astrocytes in the CUMS group when compared with that of the control. Notably, *circKat6b* overexpression attenuated the nuclear translocation of stat1 that was induced by esketamine treatment. Similarly, *circKat6b* overexpression in the hippocampus via AAV infection partially attenuated the esketamine-induced increase in astrocyte count (Fig. 6C).

Discussion

Similar to ketamine, the routine use of esketamine in daily medical practice is hindered by adverse effects, including transient dissociative and psychotic symptoms [5]. Therefore, uncovering the molecular mechanisms underlying the antidepressant activities of esketamine/ketamine and identifying potential downstream therapeutic targets are promising for the treatment of major depressive disorders. In the present study, we present the first characterization of *circKat6b*, a newly identified exon-derived circular RNA that is highly conserved and expressed in astrocytes. Furthermore, we demonstrate that *circKat6b* plays a crucial role in mediating the antidepressant effects of esketamine. *CircKat6b* responds to esketamine/ketamine treatment, suggesting it

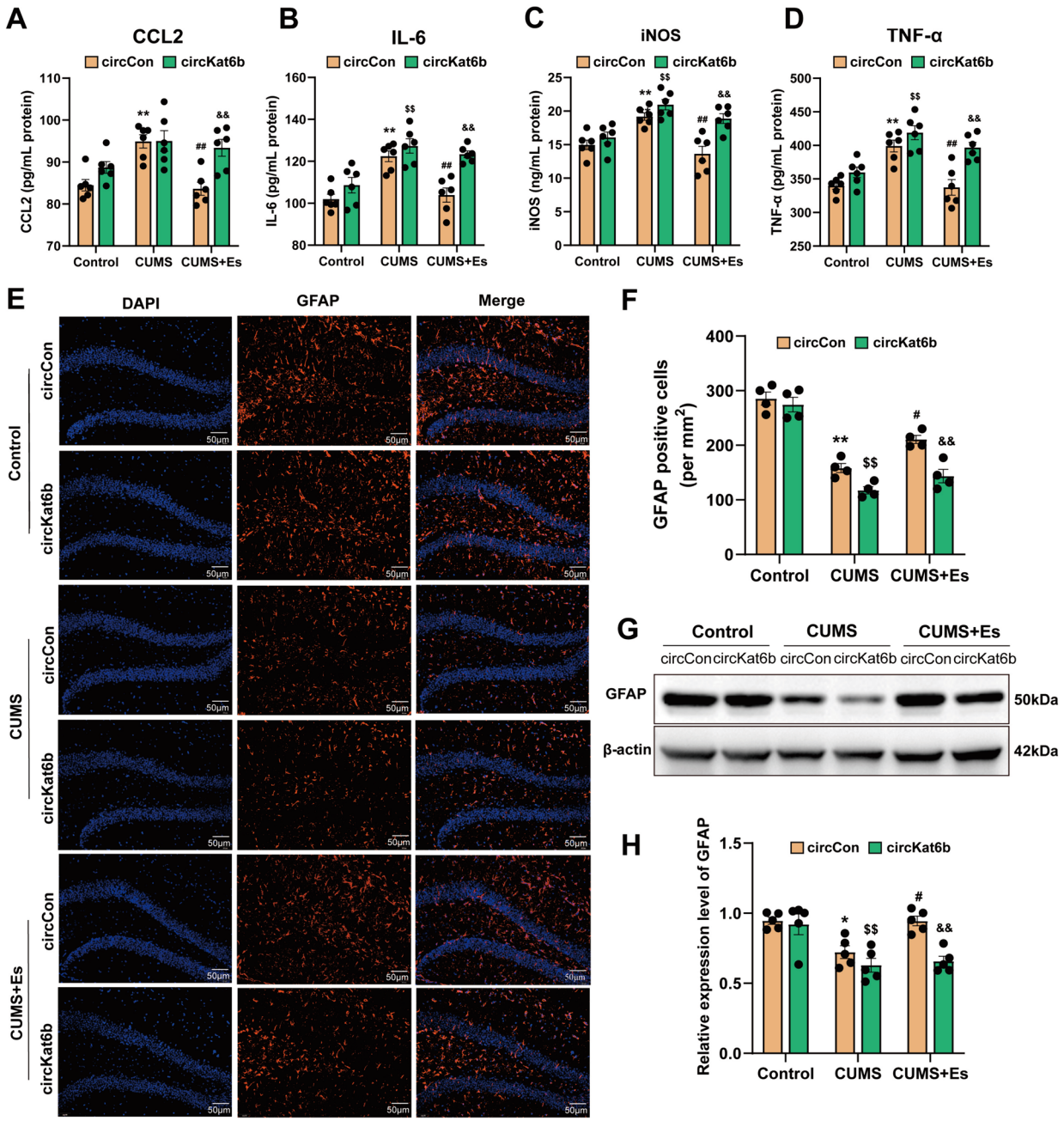

Fig. 4 Effect of *circKat6b* on hippocampal astrocyte function in CUMS mice. **A**–**D** Effect of overexpression of *circKat6b* on inflammatory factors in the hippocampus was measured using ELISA ($N=6$). **E** Representative immunohistochemical images of astrocytes expressing GFAP in the mouse hippocampus. Scale bar = 50 μm. **F** Quantification of GFAP-positive cells per mm^2 in the mouse hippocampus; $N=4$. **G**, **H** Protein expression of GFAP in the hippocampus ($N=6$), vs control-circCon group, $^{*}P<0.05$, $^{**}P<0.01$; vs control-circKat6b group, $^{\$\$}P<0.01$; vs CUMS-circCon group, $^{\#}P<0.05$, $^{\#\#}P<0.01$; vs CUMS + Es-circCon group, $^{\&\&}P<0.01$ using two-way ANOVA followed by Tukey's test

may be a potential therapeutic target and diagnostic strategy for patients with depression.

CircRNAs are present in many types of tissues, exosomes, and bodily fluids, including blood, urine, cerebrospinal fluid, and saliva [31]. Given their abundance and high stability, circRNAs have a remarkable potential as biomarkers for disease diagnosis, monitoring, and prognostication [32]. *CircKat6b* has a high degree of homology among mice, rats, and humans, and its circular structure is relatively stable against RNase R degradation. The properties of circRNAs determine their important roles in transcription and post-transcription processes. Evidence suggests that precursor

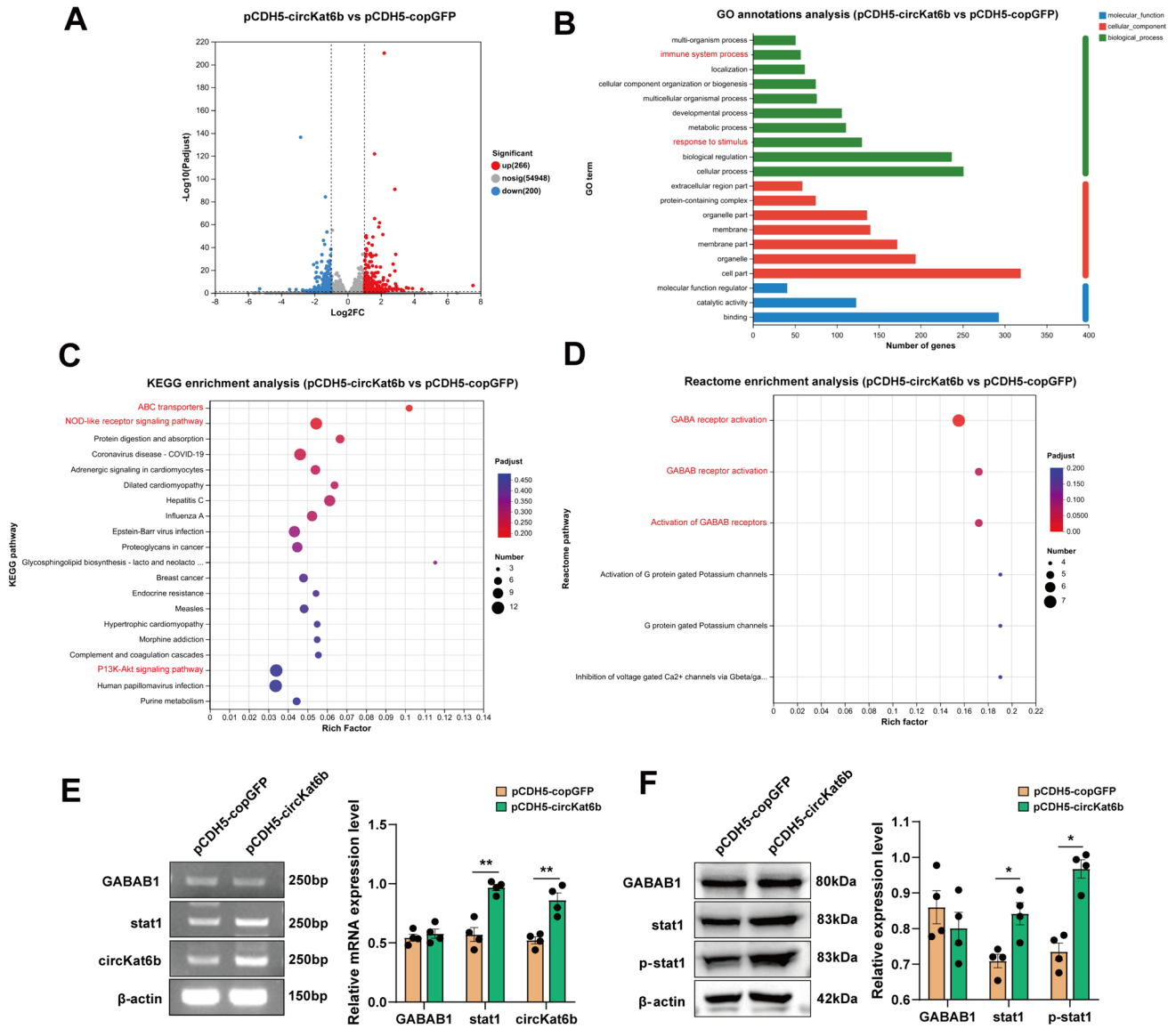

Fig. 5 Differential expression and functional analysis in astrocytes overexpressing *circKat6b*. **A** Volcano map of DEGs in the pCDH5-circKat6b vs pCDH5-copGFP where red represents upregulated genes and blue represents downregulated genes. **B** GO (CC, MF, BP) classification, **C** KEGG pathway analysis, and **D** reactome enrichment analysis of DEGs related to *circKat6b* overexpression. **E** RT-PCR results of *GABAB1*, *stat1*, and *circKat6b* mRNA in C8D1A overexpressing *circKat6b*. **F** Western blot results of GABAB1, stat1, and p-stat1 in C8D1A overexpressing *circKat6b*. $N=4$, vs pCDH5-copGFP group, $^{*}P<0.05$, $^{**}P<0.01$ using Student's *t*-test

mRNAs originating from spliced exon or intron sequences can generate different circRNAs, with the former primarily localized in the cytoplasm and the latter in the nucleus [33]. *CircKat6b* is circularized from the *Kat6b* exon 2 in mice and is localized primarily in the cytoplasm of astrocytes. In this study, we observed an upregulation of *circKat6b* expression in the hippocampus of mice subjected to CUMS, whereas esketamine treatment resulted in the downregulation of *circKat6b* expression and a significant improvement in the depressive-like behavior of the CUMS mice. Moreover, the overexpression of *circKat6b* significantly reduced the antidepressant effects of esketamine, suggesting that *circKat6b* mediated the antidepressant effects of esketamine. It should be noted that existing literature suggests that motor activity may be changed by hippocampal function [34–36]. As this study did not evaluate the effect of *circKat6b*-AAV overexpression in the hippocampus on locomotor activity of mice, the results obtained in FST and TST may be influenced by the change in spontaneous activity of mice, which was a limitation of this study. There is substantial evidence indicating that circRNAs are involved in the pathogenesis of depression and their significance in

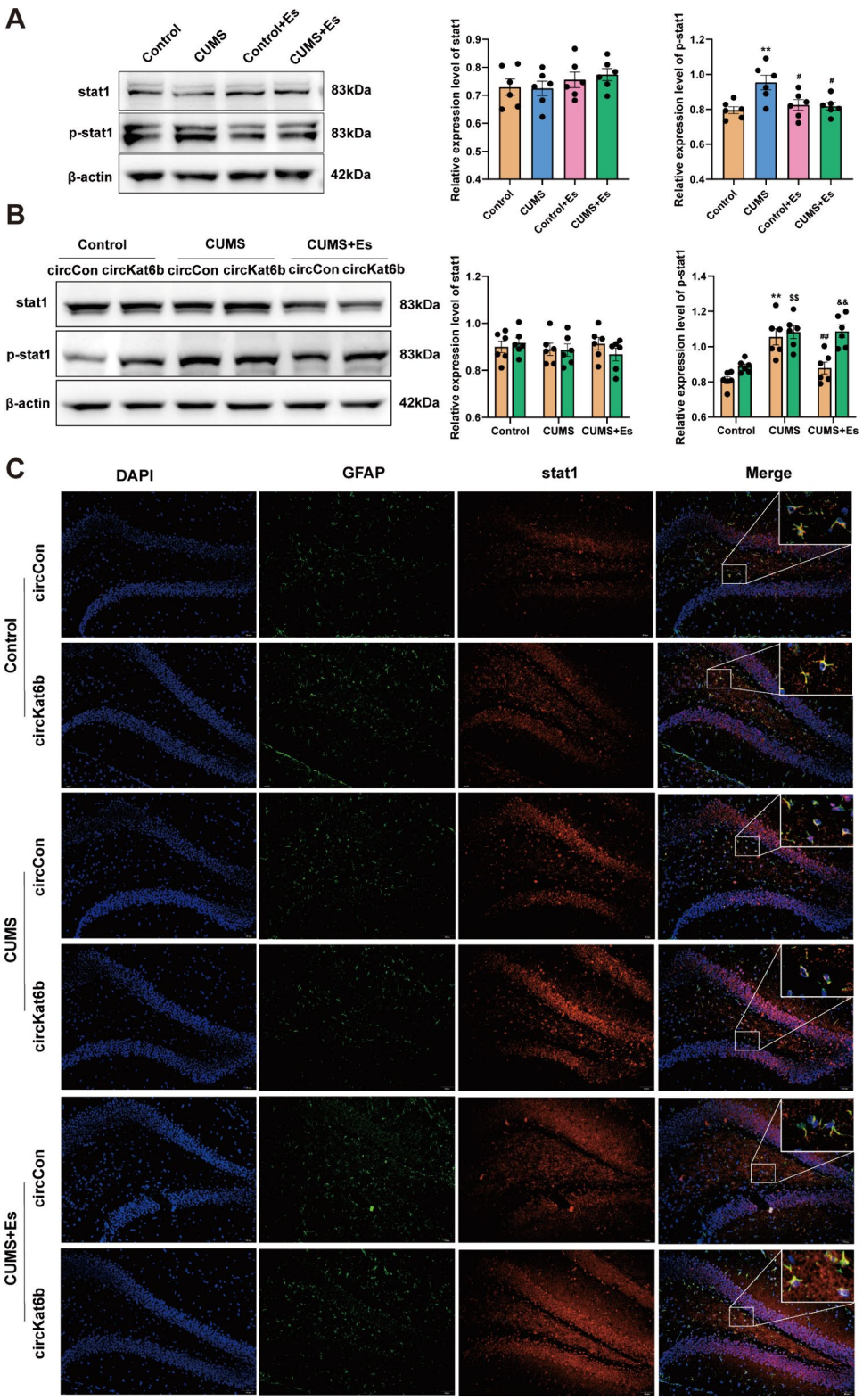

Fig. 6 *CircKat6b* regulates astrocyte function via stat1. **A** Protein expression of stat1 and p-stat1 protein in the hippocampus in each group. $N=6$, vs control group, $^{**}P<0.01$; vs CUMS group, $^{\#}P<0.05$ using one-way ANOVA followed by Tukey's test. **B** Effect of *circKat6b* overexpression on stat1 and p-stat1 protein expression in the hippocampus in each group. $N=6$, vs control-circCon group, $^{**}P<0.01$; vs control-circKat6b group, $^{\$\$}P<0.01$; vs CUMS-circKat6b group, $^{\#\#}P<0.01$; vs CUMS + Es-circCon group, $^{\&\&}P<0.01$ using two-way ANOVA followed by Tukey's test. **C** Representative double-staining immunofluorescence of p-stat1 and GFAP in brain sections from different groups following esketamine treatment. Scale bar = 20 μm

antidepressant therapies. Zhang et al. reported that *circDYM* mitigates depression-like behaviors through its interaction with miRNA-9, leading to the regulation of HSP90 ubiquitination and subsequent microglial activation [12]. Aberrant expression of *circSTAG1* and *circHIPK2* is associated with astrocyte dysfunction and may partially induce depressive symptoms [28, 37]. In addition, the antidepressant saponins from the leaves of *Panax notoginseng* upregulate the level

of mmu-circ-0001223 to increase the expression of brain-derived neurotrophic factor (BDNF) and ultimately ameliorate depressive-like behavior in mice [38]. In conclusion, circRNAs have a substantial impact on the pathogenesis of depression and potential as biomarkers for epigenetic or pharmacological interventions in depression. However, the precise mechanisms underlying the effects of *circKat6b* on the antidepressant properties of esketamine remain elusive.

Previous studies have demonstrated the significant involvement of astrocytes in the pathophysiological mechanisms underlying depression, indicating that they are potential candidates for screening novel antidepressant medications [39, 40]. Astrocyte dysfunction in depression is characterized by various alterations including diminished cell density, anomalous morphology (e.g., decreased branch length, volume, and number), decreased GFAP expression, and aberrant membrane channel function [41]. Antidepressant administration can reduce neuronal apoptosis within the hippocampus and decrease the secretion of pro-inflammatory factors IL-1β, IL-6, and TNF-α by astrocytes and microglia [42, 43]. These findings are consistent with our experimental results that the expression of IL-6, TNF-α, iNOS, and CCL2 were significantly upregulated in the hippocampus of depressive-like mice administered CUMS, and this alteration was reversed by esketamine treatment. Overexpression of *circKat6b* effectively attenuated the esketamine-induced effects, including inflammatory factor expression in CUMS mice. Furthermore, improvement in the number of astrocytes in the hippocampus was concomitant with GFAP protein expression level. These results suggest that *circKat6b* may affect depression-like behavior in mice by modulating astrocyte function.

To elucidate the precise mechanism underlying *circKat6b*-induced astrocyte dysfunction, we performed an RNA-seq analysis. The DEGs in response to *circKat6b* expression were identified by comparing the pCDH5-copGFP and pCDH5-circKat6b groups. GO, KEGG, and reactome analyses revealed that these DEGs were significantly enriched in pathways related to cell growth, energy metabolism, immune-inflammatory responses, and GABA receptor activation. The gene *stat1* was upregulated in *circKat6b*-expressing cells, which exhibited a significantly enriched immune-inflammatory response pathway. Conversely, *GABAB1*, which is predominantly enriched in the GABA receptor activation pathway, was downregulated in response to *circKat6b* expression. We also identified significant differences in the gene and protein expression of stat1 and p-stat1, suggesting that stat1 may serve as a downstream target for *circKat6b* action.

The JAK2/STAT1 signaling pathway is an extensively preserved inflammatory pathway that is strongly correlated with neuronal cell activation, synaptic plasticity, and modulation of cognitive functions [44]. The expression of stat1 significantly increased in whole blood tests conducted on patients with treatment-resistant depression [45]. Activation of stat1 in the hippocampal tissue of depressed mice induced by lipopolysaccharides (LPS) leads to neuroinflammation, suggesting an important role for stat1 the pathogenesis of depression [46]. We found that p-stat1 expression increased in the CUMS mouse model and subsequently decreased following esketamine administration. However, *circKat6b* overexpression significantly attenuated esketamine-induced downregulation of p-stat1 in the CUMS mouse model, further suggesting that stat1 may serve as a putative regulator

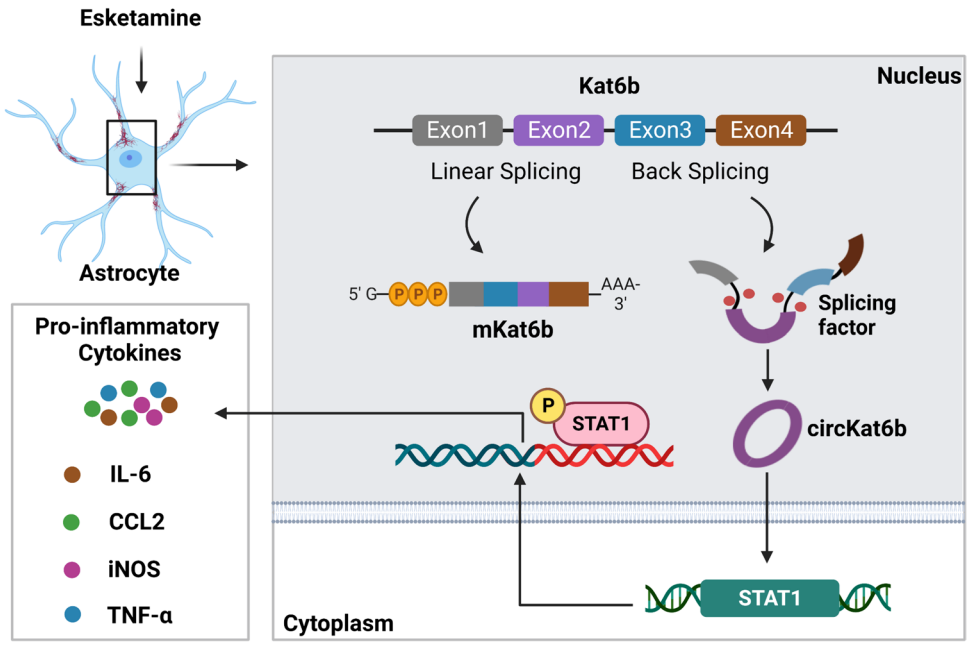

Fig. 7 A schematic diagram depicting how esketamine affects the function of astrocytes through the regulation of stat1 expression via *circKat6b* to exert an antidepressant effect

of the pathogenesis and maintenance of depression. Upon phosphorylation, stat1 undergoes polymerization, resulting in the formation of an activated transcription activator that can translocate to the nucleus and bind specific target genes to facilitate their transcription [47]. Stat1 activation is implicated in cellular responses to pro-inflammatory cells such as IL-1 and TNF-α, as well as growth factors and immunomodulatory proteins [48]. Furthermore, stat1 activation induces astrocytes to produce adhesion molecules (e.g., ICAM-1/VCAM-1), inflammatory factors (e.g., TNF, IL-6), and chemokines (e.g., CCL2, CXCL8, and CXCL10) to initiate inflammatory responses within the nervous system to exert its regulatory function [22, 23]. Immunofluorescence results highlighted the enrichment of stat1 in astrocytes, along with significant nuclear location of stat1 in the CUMS mouse model, concomitant with a reduction in the astrocyte population. Conversely, the overexpression of *circKat6b* attenuated the nuclear translocation of stat1 induced by esketamine treatment. These findings indicate a potentially significant correlation between stat1 activation and astrocyte dysfunction, identifying stat1 is a promising target for antidepressant intervention, although further investigation is necessary to validate this hypothesis.

CircRNAs function through the following mechanisms: (1) as a "sponge" that absorbs miRNAs in the cytoplasm [49], (2) interacting with RNA-binding proteins (RBPs) in the cytoplasm [50], (3) regulating parental gene expression in the nucleus [51], and (4) translating novel peptides [52]. Given that *circKat6b* is predominantly localized in the cytoplasm of astrocytes, it is plausible that it regulates the expression level of *stat1* by sponging miRNAs, interacting with RBPs, and participating other regulatory mechanisms. Consequently, this modulation influences the functionality of astrocytes and implicates their involvement in the progression of depression. Elucidating these aspects of *circKat6b* function will be the focus of our forthcoming experiments.

In conclusion, this study successfully established a novel functional association between esketamine and *circKat6b* expression. Specifically, esketamine administration downregulated *circKat6b* expression in astrocytes within the hippocampus of a depression-like mouse model, leading to reduced stat1 phosphorylation and enhanced astrocyte functionality, ultimately exerting antidepressant effects (Fig. 7). Therefore, *circKat6b* has emerged as a promising target for the diagnosis and treatment of depression and provides valuable insights into preventive strategies and effective diagnostic and therapeutic approaches for depression.

Supplementary Information The online version contains supplementary material available at https://doi.org/10.1007/s12035-024-04420-0.

Author Contribution "W.X.B., F.J.G., L.L.and Z.C.X designed the conceptualization and methodology; H.N., L.X.R., Z.Y.J. and J.J. performed the formal analysis and investigation; H.N. and L.X.R. wrote the main manuscript and prepared figures; W.X.B. wrote and edited the manuscript. All authors reviewed the manuscript."

Funding This work was supported by the Department of Science and Technology of Sichuan Province, China (Grant No. 2022YFS0632), and Scientific research project of Luzhou Science and Technology Bureau, China (2021LZXNYD-Z06).

Data Availability No datasets were generated or analysed during the current study.

Declarations

Competing Interests The authors declare no competing interests.

References

1. Charlson F, van Ommeren M, Flaxman A, Cornett J, Whiteford H, Saxena S (2019) New WHO prevalence estimates of mental disorders in conflict settings: a systematic review and meta-analysis. Lancet (London, England) 394(10194):240–248. https://doi.org/10.1016/s0140-6736(19)30934-1
2. Duman RS, Aghajanian GK (2012) Synaptic dysfunction in depression: potential therapeutic targets. Science (New York, NY) 338(6103):68–72. https://doi.org/10.1126/science.1222939
3. McIntyre RS, Rosenblat JD, Nemeroff CB, Sanacora G, Murrough JW, Berk M, Brietzke E, Dodd S et al (2021) Synthesizing the evidence for ketamine and esketamine in treatment-resistant depression: an international expert opinion on the available evidence and implementation. Am J Psychiatry 178(5):383–399. https://doi.org/10.1176/appi.ajp.2020.20081251
4. Kim J, Farchione T, Potter A, Chen Q, Temple R (2019) Esketamine for treatment-resistant depression - first FDA-approved antidepressant in a new class. N Engl J Med 381(1):1–4. https://doi.org/10.1056/NEJMp1903305
5. Singh JB, Fedgchin M, Daly E, Xi L, Melman C, De Bruecker G, Tadic A, Sienaert P et al (2016) Intravenous esketamine in adult treatment-resistant depression: a double-blind, double-randomization, placebo-controlled study. Biol Psychiatry 80(6):424–431. https://doi.org/10.1016/j.biopsych.2015.10.018
6. Maass PG, Glažar P, Memczak S, Dittmar G, Hollfinger I, Schreyer L, Sauer AV, Toka O et al (2017) A map of human circular RNAs in clinically relevant tissues. J Mol Med (Berl) 95(11):1179–1189. https://doi.org/10.1007/s00109-017-1582-9
7. Zaghlool A, Ameur A, Wu C, Westholm JO, Niazi A, Manivannan M, Bramlett K, Nilsson M et al (2018) Expression profiling

and in situ screening of circular RNAs in human tissues. Sci Rep 8(1):16953. https://doi.org/10.1038/s41598-018-35001-6
8. Hanan M, Soreq H, Kadener S (2017) CircRNAs in the brain. RNA Biol 14(8):1028–1034. https://doi.org/10.1080/15476286.2016.1255398
9. Liu CX, Chen LL (2022) Circular RNAs: characterization, cellular roles, and applications. Cell 185(12):2016–2034. https://doi.org/10.1016/j.cell.2022.04.021
10. You X, Vlatkovic I, Babic A, Will T, Epstein I, Tushev G, Akbalik G, Wang M et al (2015) Neural circular RNAs are derived from synaptic genes and regulated by development and plasticity. Nat Neurosci 18(4):603–610. https://doi.org/10.1038/nn.3975
11. Floris G, Zhang L, Follesa P, Sun T (2017) Regulatory role of circular RNAs and neurological disorders. Mol Neurobiol 54(7):5156–5165. https://doi.org/10.1007/s12035-016-0055-4
12. Zhang Y, Du L, Bai Y, Han B, He C, Gong L, Huang R, Shen L et al (2020) CircDYM ameliorates depressive-like behavior by targeting miR-9 to regulate microglial activation via HSP90 ubiquitination. Mol Psychiatry 25(6):1175–1190. https://doi.org/10.1038/s41380-018-0285-0
13. Mao J, Li T, Fan D, Zhou H, Feng J, Liu L, Zhang C, Wang X (2020) Abnormal expression of rno_circRNA_014900 and rno_circRNA_005442 induced by ketamine in the rat hippocampus. BMC Psychiatry 20(1):1. https://doi.org/10.1186/s12888-019-2374-2
14. Cao X, Li LP, Wang Q, Wu Q, Hu HH, Zhang M, Fang YY, Zhang J et al (2013) Astrocyte-derived ATP modulates depressive-like behaviors. Nat Med 19(6):773–777. https://doi.org/10.1038/nm.3162
15. Kim YK, Won E (2017) The influence of stress on neuroinflammation and alterations in brain structure and function in major depressive disorder. Behav Brain Res 329:6–11. https://doi.org/10.1016/j.bbr.2017.04.020
16. Sofroniew MV (2020) Astrocyte reactivity: subtypes, states, and functions in CNS innate immunity. Trends Immunol 41(9):758–770. https://doi.org/10.1016/j.it.2020.07.004
17. Köhler CA, Freitas TH, Maes M, de Andrade NQ, Liu CS, Fernandes BS, Stubbs B, Solmi M et al (2017) Peripheral cytokine and chemokine alterations in depression: a meta-analysis of 82 studies. Acta Psychiatr Scand 135(5):373–387. https://doi.org/10.1111/acps.12698
18. Lou YX, Li J, Wang ZZ, Xia CY, Chen NH (2018) Glucocorticoid receptor activation induces decrease of hippocampal astrocyte number in rats. Psychopharmacology 235(9):2529–2540. https://doi.org/10.1007/s00213-018-4936-2
19. Wang Y, Ni J, Zhai L, Gao C, Xie L, Zhao L, Yin X (2019) Inhibition of activated astrocyte ameliorates lipopolysaccharide-induced depressive-like behaviors. J Affect Disord 242:52–59. https://doi.org/10.1016/j.jad.2018.08.015
20. Wang L, Zhao D, Wang H, Wang L, Liu X, Zhang H (2021) FPS-ZM1 inhibits LPS-induced microglial inflammation by suppressing JAK/STAT signaling pathway. Int Immunopharmacol 100:108117. https://doi.org/10.1016/j.intimp.2021.108117
21 Maes M, Rachayon M, Jirakran K, Sodsai P, Klinchanhom S, Gałecki P, Sughondhabirom A, Basta-Kaim A (2022) The immune profile of major dysmood disorder: proof of concept and mechanism using the precision nomothetic psychiatry approach. Cells 11(7):1183. https://doi.org/10.3390/cells11071183
22. An SY, Youn GS, Kim H, Choi SY, Park J (2017) Celastrol suppresses expression of adhesion molecules and chemokines by inhibiting JNK-STAT1/NF-κB activation in poly(I:C)-stimulated astrocytes. BMB Rep 50(1):25–30. https://doi.org/10.5483/bmbrep.2017.50.1.114
23. Wang X, Deckert M, Xuan NT, Nishanth G, Just S, Waisman A, Naumann M, Schlüter D (2013) Astrocytic A20 ameliorates experimental autoimmune encephalomyelitis by inhibiting NF-κB- and STAT1-dependent chemokine production in astrocytes. Acta Neuropathol 126(5):711–724. https://doi.org/10.1007/s00401-013-1183-9
24. Feng J, Wang M, Li M, Yang J, Jia J, Liu L, Zhou J, Zhang C et al (2019) Serum miR-221-3p as a new potential biomarker for depressed mood in perioperative patients. Brain Res 1720:146296. https://doi.org/10.1016/j.brainres.2019.06.015
25. Zheng X, Wang M, Liu S, Chen H, Li Y, Yuan F, Yang L, Qiu S et al (2023) A lncRNA-encoded mitochondrial micropeptide exacerbates microglia-mediated neuroinflammation in retinal ischemia/reperfusion injury. Cell Death Dis 14(2):126. https://doi.org/10.1038/s41419-023-05617-2
26. Xu L, Ye X, Zhong J, Chen YY, Wang LL (2021) New insight of circular RNAs' roles in central nervous system post-traumatic injury. Front Neurosci 15:644239. https://doi.org/10.3389/fnins.2021.644239
27. Hu N, Chen X, Chen C, Liu X, Yi P, Xu T, Jia J, Feng J et al (2023) Exploring the role of esketamine in alleviating depressive symptoms in mice via the PGC-1α/irisin/ERK1/2 signaling pathway. Sci Rep 13(1):16611. https://doi.org/10.1038/s41598-023-43684-9
28. Huang R, Zhang Y, Bai Y, Han B, Ju M, Chen B, Yang L, Wang Y et al (2020) N(6)-Methyladenosine modification of fatty acid amide hydrolase messenger RNA in circular RNA STAG1-regulated astrocyte dysfunction and depressive-like behaviors. Biol Psychiatry 88(5):392–404. https://doi.org/10.1016/j.biopsych.2020.02.018
29 Almeida FB, Pinna G, Barros HMT (2021) The role of HPA axis and allopregnanolone on the neurobiology of major depressive disorders and PTSD. Int J Mol Sci 22(11):5495. https://doi.org/10.3390/ijms22115495
30. Ruiz NAL, Del Ángel DS, Brizuela NO, Peraza AV, Olguín HJ, Soto MP, Guzmán DC (2022) Inflammatory process and immune system in major depressive disorder. Int J Neuropsychopharmacol 25(1):46–53. https://doi.org/10.1093/ijnp/pyab072
31. Yang Q, Li F, He AT, Yang BB (2021) Circular RNAs: expression, localization, and therapeutic potentials. Mol Ther : J Am Soc Gene Ther 29(5):1683–1702. https://doi.org/10.1016/j.ymthe.2021.01.018
32. Li X, Yang L, Chen LL (2018) The biogenesis, functions, and challenges of circular RNAs. Mol Cell 71(3):428–442. https://doi.org/10.1016/j.molcel.2018.06.034
33. Dong Z, Deng L, Peng Q, Pan J, Wang Y (2020) CircRNA expression profiles and function prediction in peripheral blood mononuclear cells of patients with acute ischemic stroke. J Cell Physiol 235(3):2609–2618. https://doi.org/10.1002/jcp.29165
34. Kobayashi K, Ikeda Y, Suzuki H (2006) Locomotor activity correlates with modifications of hippocampal mossy fibre synaptic transmission. Eur J Neurosci 24(7):1867–1873. https://doi.org/10.1111/j.1460-9568.2006.05079.x
35. Bardgett ME, Henry JD (1999) Locomotor activity and accumbens Fos expression driven by ventral hippocampal stimulation require D1 and D2 receptors. Neuroscience 94(1):59–70. https://doi.org/10.1016/s0306-4522(99)00303-6
36. Mogenson GJ, Nielsen M (1984) A study of the contribution of hippocampal-accumbens-subpallidal projections to locomotor activity. Behav Neural Biol 42(1):38–51. https://doi.org/10.1016/s0163-1047(84)90412-6
37. Zhang Y, Huang R, Cheng M, Wang L, Chao J, Li J, Zheng P, Xie P et al (2019) Gut microbiota from NLRP3-deficient mice ameliorates depressive-like behaviors by regulating astrocyte dysfunction via circHIPK2. Microbiome 7(1):116. https://doi.org/10.1186/s40168-019-0733-3
38. Zhang H, Chen Z, Zhong Z, Gong W, Li J (2018) Total saponins from the leaves of Panax notoginseng inhibit depression on mouse

chronic unpredictable mild stress model by regulating circRNA expression. Brain and behavior 8(11):e01127. https://doi.org/10.1002/brb3.1127
39. Durkee C, Kofuji P, Navarrete M, Araque A (2021) Astrocyte and neuron cooperation in long-term depression. Trends Neurosci 44(10):837–848. https://doi.org/10.1016/j.tins.2021.07.004
40. Zhang HY, Wang Y, He Y, Wang T, Huang XH, Zhao CM, Zhang L, Li SW et al (2020) A1 astrocytes contribute to murine depression-like behavior and cognitive dysfunction, which can be alleviated by IL-10 or fluorocitrate treatment. J Neuroinflammation 17(1):200. https://doi.org/10.1186/s12974-020-01871-9
41. Snyder JS, Soumier A, Brewer M, Pickel J, Cameron HA (2011) Adult hippocampal neurogenesis buffers stress responses and depressive behaviour. Nature 476(7361):458–461. https://doi.org/10.1038/nature10287
42. Ali T, Rahman SU, Hao Q, Li W, Liu Z, Ali Shah F, Murtaza I, Zhang Z et al (2020) Melatonin prevents neuroinflammation and relieves depression by attenuating autophagy impairment through FOXO3a regulation. J Pineal Res 69(2):e12667. https://doi.org/10.1111/jpi.12667
43. Fang Y, Guo H, Wang Q, Liu C, Ge S, Yan B (2022) The role and mechanism of NLRP3 inflammasome-mediated astrocyte activation in dehydrocorydaline against CUMS-induced depression. Front Pharmacol 13:1008249. https://doi.org/10.3389/fphar.2022.1008249
44. Li J, Zhou Y, Du G, Qin X, Gao L (2019) Integration of transcriptomics and network analysis deciphers the mechanisms of baicalein in improving learning and memory impairment in senescence-accelerated mouse prone 8 (SAMP8). Eur J Pharmacol 865:172789. https://doi.org/10.1016/j.ejphar.2019.172789
45. Cattaneo A, Ferrari C, Turner L, Mariani N, Enache D, Hastings C, Kose M, Lombardo G et al (2020) Whole-blood expression of inflammasome- and glucocorticoid-related mRNAs correctly separates treatment-resistant depressed patients from drug-free and responsive patients in the BIODEP study. Transl Psychiatry 10(1):232. https://doi.org/10.1038/s41398-020-00874-7
46. Zheng M, Li K, Chen T, Liu S, He L (2021) Geniposide protects depression through BTK/JAK2/STAT1 signaling pathway in lipopolysaccharide-induced depressive mice. Brain Res Bull 170:65–73. https://doi.org/10.1016/j.brainresbull.2021.02.008
47. Shariq AS, Brietzke E, Rosenblat JD, Pan Z, Rong C, Ragguett RM, Park C, McIntyre RS (2018) Therapeutic potential of JAK/STAT pathway modulation in mood disorders. Rev Neurosci 30(1):1–7. https://doi.org/10.1515/revneuro-2018-0027
48. Malemud CJ, Miller AH (2008) Pro-inflammatory cytokine-induced SAPK/MAPK and JAK/STAT in rheumatoid arthritis and the new anti-depression drugs. Expert Opin Ther Targets 12(2):171–183. https://doi.org/10.1517/14728222.12.2.171
49. Han B, Zhang Y, Zhang Y, Bai Y, Chen X, Huang R, Wu F, Leng S et al (2018) Novel insight into circular RNA HECTD1 in astrocyte activation via autophagy by targeting MIR142-TIPARP: implications for cerebral ischemic stroke. Autophagy 14(7):1164–1184. https://doi.org/10.1080/15548627.2018.1458173
50. Chen J, Wu Y, Luo X, Jin D, Zhou W, Ju Z, Wang D, Meng Q et al (2021) Circular RNA circRHOBTB3 represses metastasis by regulating the HuR-mediated mRNA stability of PTBP1 in colorectal cancer. Theranostics 11(15):7507–7526. https://doi.org/10.7150/thno.59546
51. Li Z, Huang C, Bao C, Chen L, Lin M, Wang X, Zhong G, Yu B et al (2015) Exon-intron circular RNAs regulate transcription in the nucleus. Nat Struct Mol Biol 22(3):256–264. https://doi.org/10.1038/nsmb.2959
52. Chen L, Kong R, Wu C, Wang S, Liu Z, Liu S, Li S, Chen T et al (2020) Circ-MALAT1 functions as both an mRNA translation brake and a microRNA sponge to promote Self-renewal of hepatocellular cancer stem cells. Advanced Science (Weinheim, Baden-Wurttemberg, Germany) 7(4):1900949. https://doi.org/10.1002/advs.201900949